ASSESSING THE ^{14}C MARINE RESERVOIR EFFECT IN ARCHAEOLOGICAL CONTEXTS: DATA FROM THE CABEÇUDA SHELL MOUND IN SOUTHERN BRAZIL

Eduardo Q Alves[1,2,9]* • Kita D Macario[2] • Rita Scheel-Ybert[3] • Fabiana M Oliveira[2] • André Carlo Colonese[4] • Paulo César Fonseca Giannini[5] • Renato Guimarães[6] • Stewart Fallon[7] • Marcelo Muniz[8] • David Chivall[1] • Christopher Bronk Ramsey[1]

[1]Oxford Radiocarbon Accelerator Unit, Research Laboratory for Archaeology, University of Oxford, Dyson Perrins Building, South Parks Road, Oxford, OX1 3QY, UK
[2]Laboratório de Radiocarbono, Universidade Federal Fluminense, Av. Gal. Milton Tavares de Souza, s/n, Niterói, 24210-346, RJ, Brazil
[3]Laboratório de Arqueobotânica e Paisagem, Programa de Pós-Graduação em Arqueologia, Museu Nacional, Universidade Federal do Rio de Janeiro, Quinta da Boa Vista, São Cristóvão, 20940-040, RJ, Brazil
[4]Department of Prehistory and Institute of Environmental Science and Technology, Universitat Autònoma de Barcelona, Bellaterra, 08193, Spain
[5]Instituto de Geociências, Universidade de São Paulo, R. do Lago, 562, Cidade Universitária, São Paulo 05508-080, Brazil
[6]Laboratório de Difração de Raio-X, Instituto de Física, Universidade Federal Fluminense, Av. Gal. Milton Tavares de Souza, s/n, Niterói, 24210-346, RJ, Brazil
[7]Research School of Earth Sciences, Australian National University, Canberra, Australian Capital Territory, Australia
[8]Laboratório de Radioecologia e Alterações Ambientais, Instituto de Física, Universidade Federal Fluminense, Av. Gal. Milton Tavares de Souza s/n, 24210-346 Niterói, RJ, Brazil
[9]Departamento de Geoquímica, Universidade Federal Fluminense, Outeiro São João Batista, s/n, Niterói, 24001-970, RJ, Brazil

ABSTRACT. Prehistoric shell mounds can be useful for the quantification of the radiocarbon marine reservoir effect (MRE) and, at the same time, knowledge about the MRE allows for the establishment of robust chronologies for these sites. This creates a loop in which the archaeological setting has a dual role: it is part of both the method and the application. Therefore, it is paramount to address these sites from both archaeological and environmental perspectives, investigating their origin and diagenesis in order to overcome biases caused by post-depositional alterations. In this study, samples of bone, charcoal and shell from a Late Holocene shell mound in Southern Brazil, the Sambaqui de Cabeçuda, were analyzed following a multidisciplinary approach to disentangle the complex relationships between archaeology and the environment. We performed X-ray diffraction, radiocarbon dating, stable isotopes (δ^{13}C, δ^{18}O, δ^{15}N) and anthracology analyses as well as Bayesian Chronological Models and Isotope Mixing Models to assess the local MRE and to reconstruct the diet of Cabeçuda builders. Our results reveal a negative local correction for the MRE ($\Delta R = -263 \pm 46$ [14]C yr), expected for the lagoon next to the site, and diets with considerable intakes of marine proteins. We examine the implications of these results for the chronology of the site and discuss a series of complications when performing MRE studies using shell mound sites.

KEYWORDS: archaeological shell mound, coastal Brazil, radiocarbon dating, shell and bone stable isotopes, southwestern Atlantic Ocean.

INTRODUCTION

Radiocarbon (^{14}C) dating plays a fundamental role in archaeological investigations (Bayliss 2009 and references therein), but its application is not always straightforward, involving assumptions that have proved to not always be correct. Besides the correction of factors involved in the concept of a ^{14}C age *per se* (e.g., the Libby half-life), it has been pointed out that understanding the origin of carbon in a sample is key to the correct interpretation of ^{14}C chronologies. Among other factors, this is hindered by the existence of the so-called reservoir effects (Stuiver and Polach 1977), of which archaeology has mainly suffered from the marine reservoir effect (MRE), primarily due to the importance of marine-brackish material for radiocarbon dating, such as mollusk shells, which are abundant in many archaeological sites.

---

*Corresponding author. Email: eduardoa@id.uff.br

Water displaced from the surface ocean undergoes ^{14}C decay without replenishment. Considering the deep ocean residence times of the order of thousands of years (e.g., Sigman and Boyle 2000), these water masses can "age" significantly when compared to the coeval atmosphere, a phenomenon known as the MRE. This is not to say, however, that the MRE is absent at the ocean surface. Surface water contains both old carbon, derived from its interaction with deeper layers, and newly acquired carbon from the atmosphere. A practical implication of the MRE is that marine materials yield overestimated ^{14}C ages. The anomalies can reach thousands of years and the ^{14}C ages obtained from these samples are termed apparent ages (Mangerud 1972). For the present study, the relevant MRE offsets are R and ΔR, as first defined by Stuiver et al. (1986) and summarized in Alves et al. (2018). Briefly, the former represents the difference in ^{14}C age between the ocean and the atmosphere at a given time, while the latter is the ^{14}C age offset between the local and the global ocean. Unfortunately, the process of MRE quantification inherits complications of the ^{14}C dating analyses and common issues (e.g., post-depositional effects) are directly implicated in the calculation of such variables. Some of these complications, and the accessory techniques used to overcome them, are discussed in the next paragraphs for carbonate, charcoal and bone samples.

A sample is considered to be contaminated whenever, after deposition, processes other than radioactive decay change its carbon isotopic ratio; any carbon that was not initially part of the sample matrix is defined as a contaminant (Gillespie 1984; Taylor 1987). Isolating the pristine sample has been a challenge since the early developments of the radiocarbon dating technique (Libby 1954). In the case of mollusk shells, diagenesis may lead to carbonate dissolution, accompanied by recrystallization and the substitution of the original crystal structure, possibly affecting even the most interior layers of a sample (Taylor 1987). Such reactions, known as neomorphisms, take place in the presence of water via mechanisms of dissolution and precipitation (Tucker and Wright 1990), showing their strong dependence upon the deposition environmental conditions (Douka et al. 2010, and references therein). The less soluble/more stable calcium carbonate ($CaCO_3$) polymorph low-magnesium calcite (LMC, 0-4% $MgCO_3$) is preferentially crystallized after the dissolution of the metastable polymorphs high-magnesium calcite (HMC, >4% $MgCO_3$) and aragonite (Reid and Macintyre 1998, and references therein). Nevertheless, although unusual, isomineralogic diagenetic changes (aragonite to aragonite recrystallization) are also possible (see e.g., Enmar et al. 2000; Webb et al. 2007). Aragonite is the principal mineral component of shell carbonates in most species (Taylor 1987; Douka et al. 2010). Therefore, the presence of calcite in such shells is an indicator of contamination by recrystallization. Although the secondary phase may be contemporary with the original shell carbonate or even derived from its dissolution-recrystallization process, in which cases it would not represent a contaminant for the ^{14}C dating of the material, there is always the possibility of material of younger/older age in the immediate environment influencing the isotopic composition of the secondary phase (Taylor 1987; Douka et al. 2010). A powdery or "chalky" appearance can be associated with recrystallization in regions where the rate of aragonite dissolution is higher than that of calcite precipitation (Aitken 1990; McGregor and Gagan 2003) and procedures such as staining methods (e.g., Feigl 1958; Friedman 1959) and X-ray diffraction (XRD) (see e.g., Als-Nielsen and McMorrow 2011) can be used to detect secondary calcite (e.g., Chappell and Polach 1972; Sepulcre et al. 2009; Douka et al. 2010).

Charcoal samples may also yield apparent ages. This is because ^{14}C dating determines the time elapsed since the cessation of carbon exchanges between sample and environment. Therefore,

the association of this event with the context to be dated must be careful (see Waterbolk 1971). In archaeology, charcoal remains collected from hearths are often radiocarbon dated to establish a chronology for domestic and ceremonial activities. Although this approach assumes that the burning happened immediately or shortly after wood formation, this is not always the case and ages may be largely overestimated if charcoal is derived from the heartwood of long-lived species (e.g., oak) or if the death of the tree significantly pre-dates its use as fuel. In both cases, this inbuilt age is a consequence of the so-called old-wood effect and leads to uncertainties of up to hundreds of years (McFadgen 1982; Schiffer 1986; Gavin 2001). Since the old-wood effect does not affect structures such as bark, twigs, and seeds, the ^{14}C dating of these materials is usually preferred (e.g., Albero et al. 1986; Anderson 1991; Erlandson et al. 1996; Facorellis 1998; Rieth et al. 2011; Wilmshurst et al. 2011; Deforce et al. 2013). One way of identifying short-lived plant species or structures in the charcoal assemblage is the use of anthracological analyses (e.g., Vernet 1999; Scheel-Ybert 2001; Ludemann et al. 2004; Emery-Barbier and Thiébault 2005; Byrne et al. 2013; Moskal-del Hoyo 2013; Euba et al. 2016; Macario et al. 2021). By comparing the wood anatomic features preserved in charcoal with a reference collection and the specialized literature (e.g., Metcalfe and Chalk 1950; Scheel-Ybert 2016 2020), it is possible to taxonomically classify charcoal fragments and thus avoid the old-wood effect.

Finally, the radiocarbon dating of bone samples also needs to be performed with caution. The recognition that, owing to a mixed marine/terrestrial diet, materials traditionally considered as terrestrial, such as human bone, could also be affected by the MRE is important for the establishment of accurate chronologies for archaeological sites. This type of sample yields a partially marine ^{14}C age, which depends on the proportion of marine-derived carbon in the material, that must be calibrated with mixed marine/atmospheric calibration curves and the appropriate MRE correction (see e.g., Beavan and Sparks 1998; Arneborg et al. 1999; Beavan-Athfield et al. 2001; Naito et al. 2010; Commendador 2014; Ervynck 2014; Cook et al. 2015). For human bones, stable isotope analyses can provide an estimation of the relative contribution of marine resources to diet. Stable carbon isotope measurements can be used for diet analyses and allow for the quantification of the relative contribution of different food classes from the same (e.g., C3 vs. C4 plants) or distinct (e.g., marine vs. terrestrial species) environments (e.g., Van de Merwe 1982; Chisholm et al. 1982; Schwarcz et al. 1985; Walker and DeNiro 1986; Ambrose 1986). However, complications in dietary estimations may arise from the fact that diet-to-tissue isotopic fractionation and the relative contribution of carbon isotopes from different food sources will depend on the nature of the diet (Webb et al. 2017; Jim et al. 2006). Stable isotopes of nitrogen are passed along food webs with relatively well-established fractionations, e.g., 3–6‰ (Schoeninger et al. 1983; O'Connell et al. 2012) and can differentiate between herbivores (low trophic position) and carnivores (high trophic position) or between marine and terrestrial food webs (e.g., Schoeninger et al. 1983; Schoeninger and DeNiro 1984; Walker and DeNiro 1986). Nevertheless, there are environmental and physiological factors influencing nitrogen isotope ratios which limit dietary interpretations based on these values only (see e.g., Hedges and Reynard 2007).

The presence of marine and terrestrial material in close stratigraphic association at coastal archaeological sites along the Brazilian shoreline makes it possible to derive marine reservoir corrections for the region. In order to yield meaningful MRE quantifications, stratigraphic pairing must be a reliable indicator of contemporaneity. Moreover, the validity of such an approach relies on the consideration of possible obstacles such as the old-wood effect and the recrystallization issues discussed above. Here, by analyzing
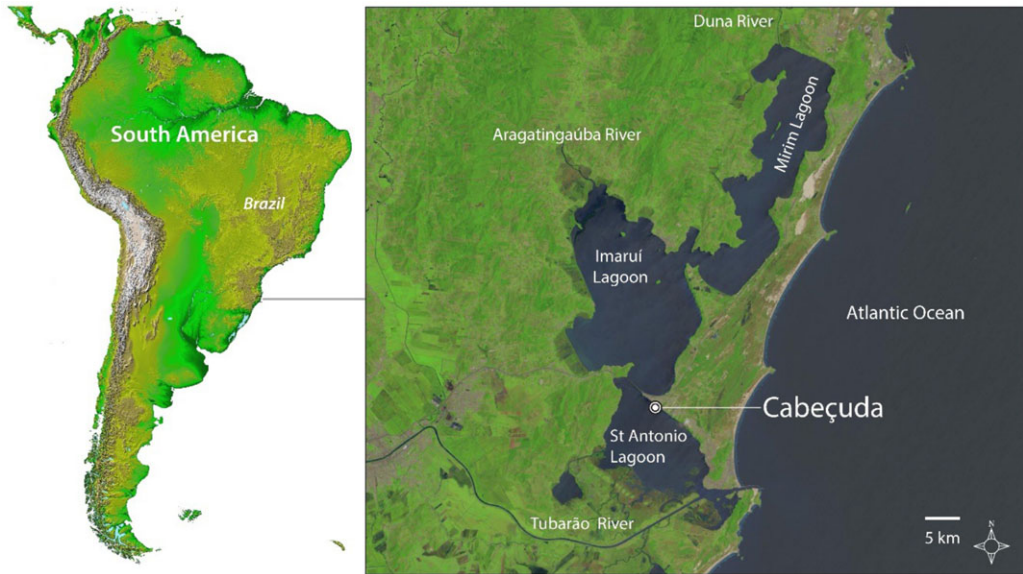
Figure 1   Laguna Lagoonal System (LLS) in southern Brazil and the location of Cabeçuda. Satellite imagery from USGS (Earth Explorer) and NASA (Shuttle Radar Topography Mission).

lagoonal-brackish (shell) and terrestrial (charcoal) materials from the archaeological context of a Southern Brazilian shell mound, we describe what we consider to be the best practices for overcoming these issues.

MATERIALS AND METHODS

The Cabeçuda Shell Mound

The Brazilian coastline is well known for bearing a great number of archaeological shell mounds. Sambaqui (Tamba = shell, ki = heap) is a word of Tupi etymology used to designate this type of site, usually found near large bodies of water (e.g., Gaspar et al. 2008). The prehistoric groups who built coastal sambaquis are depicted as fishers and gardeners that occupied and harvested the rich terrestrial, estuarine and marine environments of the Brazilian littoral (Lima 2000; Wagner et al. 2011; Scheel-Ybert and Boyadjian 2020; Toso et al. 2021). The sambaquis were monumental funerary constructions where extremely elaborate rituals and feastings took place (DeBlasis et al. 2007; Villagran and Giannini 2014; Kneip et al. 2018; Scheel-Ybert et al. 2020). In this context, the Sambaqui de Cabeçuda, in Southern Brazil, stands out as an important coastal site, due to its key location in the landscape, monumentality associated with the funerary ritual, and the long duration of its occupation (Figure 1). It was the first sambaqui of large dimensions to be systematically investigated and its abundance and diversity of archaeological remains place it in a special position in Brazilian archaeology (Klokler 2014; Scheel-Ybert et al. 2020).

Cabeçuda is situated in the state of Santa Catarina, between the Santo Antônio dos Anjos and the Imaruí lagoons (UTM 22J 712601-6852170 SAD69), in a region of high sambaqui density (Rodrigues-Carvalho and Mendonça de Souza 1998; DeBlasis et al. 2007; Klokler 2014;

Kneip et al. 2018). Together with the Mirim lagoon, these two lagoons form the Laguna Lagoonal System (LLS) that covers an area of 180 km^2. The lagoons are connected by narrow channels and receive a significant amount of their inflow from the three main rivers in the region: the Tubarão, the D'Una and the Aratingaúba rivers (Giannini 2002). The former discharges in the Santo Antônio dos Anjos lagoon while the Imaruí and Mirim lagoons receive freshwater from the others (Fonseca and Netto 2006) (Figure 1). Kjerfve (1994) classifies this system as a choked lagoon, connected to the sea by a single entrance channel that contributes to the greater salinity of the Santo Antônio dos Anjos lagoon when compared to the other two. In fact, the north portion of this lagoon complex presents salinity < 0.5 during the entire year, while the middle lagoon has a salinity of 0.5–5, mostly influenced by rainfall patterns (Barletta et al. 2017, and references therein). In the past, the higher salinity of the Santo Antônio lagoon may have also been influenced by a lagoonal inlet, which is presently almost closed, in the southern portion of the LLS (Giannini 1993; Tanaka et al. 2009; Giannini et al. 2010; Fornari et al. 2012). The mean depth of the system is approximately 2 m, meaning that wind can significantly influence circulation. Much of the tidal influence is filtered out by the narrow channel that connects the ocean and the Santo Antônio dos Anjos lagoon (Fonseca and Netto 2006). There is geological evidence that the LLS was formed by the submersion of incised valleys parallel to the coast during early to mid-Holocene, under a sea-level higher than that of the present day (Giannini 2002; Giannini et al. 2007, 2010; Amaral et al. 2012). This happened due to post-glacial sea-level rise (Angulo et al. 1999, 2006); at the time, the LLS was connected with a wide bay to the southwest, where oceanic circulation was more direct. At about 6 ka cal BP, due to the formation and progressive widening of a sand barrier, this paleobay to southwest gradually changed to its present configuration of coastal lagoons (the Santa Marta, Camacho and Garopaba do Sul lagoons) (Tanaka et al. 2009; Giannini et al 2010; Amaral et al. 2012; Fornari et al. 2012). Since then, the entry of sea water has been restricted to two inlets, the intermittent one in Camacho, about 18 km southwest of Cabeçuda, and the permanent one in Entrada da Barra, 7 km southeast and in the southern portion of Santo Antônio dos Anjos lagoon.

The Sambaqui de Cabeçuda rests partly on sandy sediments of an eolian paleodune (belonging to generation G2 described in Giannini et al. (2007), dominant previous or contemporaneous to the Holocene maximum flooding) whose reddish-brown color is due to the presence of post-depositional silty clay, and partly on a pink granite of the Precambrian basement (Guerra 1950, Giannini et al. 2007). In its original size, Cabeçuda was estimated to have been 22 m in height, 400 m in diameter and 53,000 m^3 in volume (Rohr 1961; Mendonça de Souza 1995; Klokler 2014). Currently, due to urban expansion and historical exploitation for lime production, less than 25% of the original site volume is preserved (Klokler 2014; Scheel-Ybert et al. 2020, and references therein) (Figure 2). Nevertheless, Cabeçuda remains a key site for the reconstruction of the paleoenvironment and the understanding of the social dynamics of sambaqui builders in southern Brazil. Excavations in this site resumed recently and several field campaigns took place from 2010 to 2017. The site presents a complex stratigraphy, showing an alternation of light-colored shellfish-rich layers and dark organic layers. In the former, fish bones and charcoal were found scattered. In the latter, compact sandy sediments predominated over shellfish remains, burials were present, and fish bones, charcoal, and lithic artefacts were abundant. These layers were less thick and covered by the shellfish layers. High concentrations of fish bones found in funerary contexts suggest the presence of offerings, while large charcoal deposits associated with the burials indicate the importance of fire in the funerary ritual (Scheel-Ybert et al. 2020).
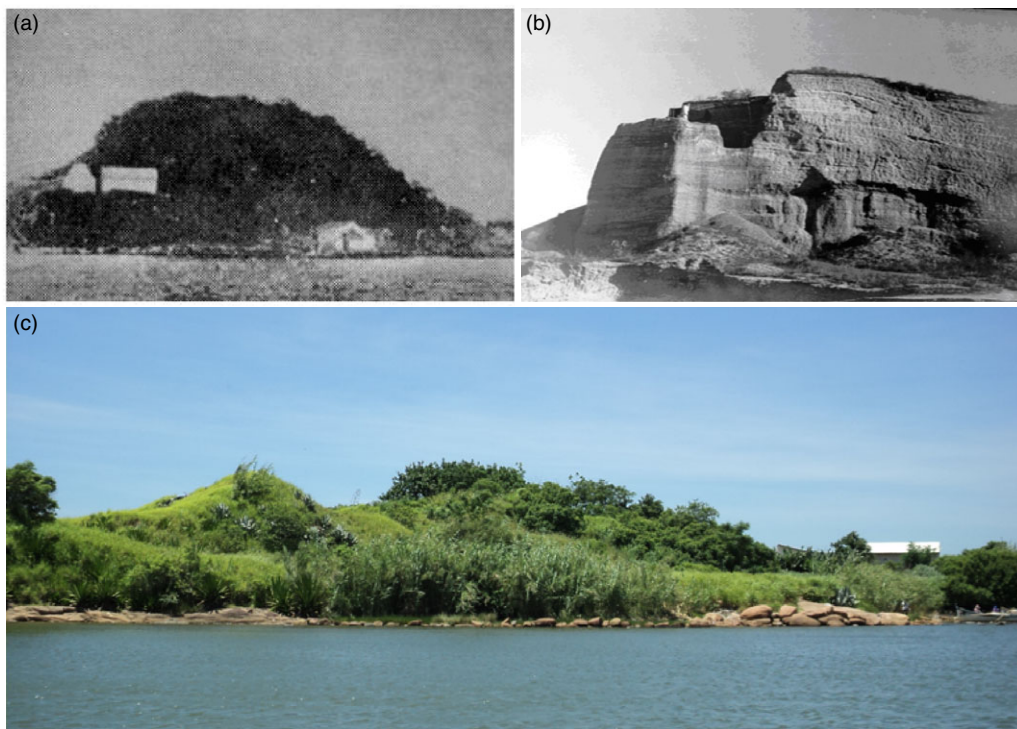
Figure 2   Cabeçuda in 1928 (a), at the time of the first excavation in 1950 (b), and at the time of the second excavation in 2012 (c) (Photos: S. Fróes de Abreu, L. Castro Faria, R. Scheel-Ybert, respectively).

The Sample Set

Samples used in the present study, including shell, charcoal and bone were directly associated with five different burials recovered in the 2010–2012 excavations (see Supplementary Material for a description of the burials). The contemporaneity of the samples is a fundamental requirement for the derivation of ΔR values. The specimens used in this research are coeval samples, retrieved from the same archaeological contexts. The samples were taken from burial features, consisting of bones from the burial itself along with associated samples of shell and charcoal which are related to the funerary ritual (Scheel-Ybert et al. 2020). Three different contexts were analyzed. Two of them are situated in locus 1, in the northwestern part of the site: burials E1, E3, and E5 come from the same funerary area, where a horizontal excavation of 20 m^2 was performed by decapage, and are most likely contemporaneous by a few days, years or decades (although burial E5 is necessarily younger than burial E1, for it was deposited just above it); burials P6 and P7 come from different archaeological layers from the profile beneath this funerary area. Burial P7, stratigraphically lower, is situated ca. 40 cm below burial P6; this one is situated ca. 1.30 m below the excavation area where the other burials were found. The later context refers to burial P13, which comes from locus 2, presently situated in the middle part of the site, ca. 25 m apart from locus 1. This burial is situated at around the same height as burials P6 and P7. However, their contemporaneity cannot be inferred stratigraphically alone, because different areas of the site were established at the same time; the building of the site did not happen linearly, but according to several events carried out in distinct places (Scheel-Ybert et al. 2020).

Analyses

Anthracological and Malacological Analyses

Charcoal samples were subjected to anthracological investigations to rule out the old-wood effect. These analyses were performed at the Archaeobotany and Landscape Laboratory of the National Museum of Brazil – Universidade Federal do Rio de Janeiro (LAP-MN/ UFRJ). Samples were manually broken, exposing the three fundamental wood sections (transversal, tangential longitudinal, and tangential radial), and examined under a reflected light brightfield/darkfield microscope. Anatomical structures were then exhaustively compared to a well-identified comparative collection (charcoal collection from Museu Nacional, UFRJ; Scheel-Ybert et al. 2016), allowing taxonomic identification. Additionally, descriptions and photographs from the specialized literature (e.g., Metcalfe and Chalk 1950; Detienne and Jacquet 1983) were consulted to support the identifications. A large set of charcoal samples was analyzed and structures such as barks and twigs were selected to avoid the old-wood effect. In the absence of those, charcoal pieces derived from branches of restinga taxa (Myrtaceae, Sapotaceae, Leguminosae, Sapidaceae, and Rutaceae), which are not usually composed of long-lived species, were selected.

The restinga vegetation is a mosaic of plant associations with diverse physiognomies typical to sandy beach and foredune ridges. It consists of an extremely dynamic ecosystem which is (and has been) in constant change and remodeling due to eolian and marine processes, including sea-level variations (see Scheel-Ybert and Boyadjean 2020, and references therein). Therefore, the restinga flora is mainly composed by pioneer and early secondary species, which usually have a short life spam. Typically, pioneer species do not exceed ten years of age and early secondary species, 10–25 years (Budowski 1965).

The archaeological shells obtained for the present study were identified to species level with the support of the specialized literature (e.g., de Souza et al. 2011) and a reference collection. Shells of the suspension-feeder bivalve *Anomalocardia flexuosa* (Linnaeus 1767) were selected. This organism tolerates large variations in salinity (> 17) and is geographically widespread (Abbott 1974; Leonel et al. 1983; Monti et al. 1991; Rios 1994; Rodrigues et al. 2013), typically inhabiting environments protected from the wave action, such as mangroves, estuaries, muddy beaches, and intertidal zones (Boehs and Magalhães 2004; de Souza et al. 2011). This means that these shells were most probably collected from the lagoons adjacent to Cabeçuda.

X-Ray Diffraction

In order to assess the potential for shell recrystallization, the archaeological shells were analyzed using X-ray Diffraction (XRD) at the Laboratory of the Universidade Federal Fluminense (LDRX-UFF). Samples were homogenized with a mortar and pestle, and the fine powder was analyzed in a Bruker AXS D8 Advance (Cu Kα radiation, 40 kV, 40 mA) diffractometer. The machine was operated in a Bragg–Brentano θ/θ configuration with the diffraction patterns being collected in a flat geometry with steps of 0.02 degrees and accumulation time of 2.0 s per step using a PSD detector (Bruker AXS LynexEye model). Data were refined following the Rietveld method and using the GSAS-II software (Toby and Von Dreele 2013).

Stable Isotopes Analyses

Bone collagen $\delta^{13}C$ and $\delta^{15}N$ analyses were performed on five human individuals for dietary reconstructions and for assessing the relative contribution of marine carbon in bone collagen.

Samples were analyzed at the Oxford Radiocarbon Accelerator Unit (ORAU, University of Oxford, UK) following the collagen extraction protocol proposed by Brock et al. (2010). Stable isotope analyses were performed with an aliquot of the gas used for ^{14}C dating. Collagen samples (2–5 mg) were analyzed using a continuous flow isotope ratio mass spectrometer composed of a combustion elemental analyzer (Carlo-Erba NA 2000) and a gas source isotope ratio mass spectrometer (IRMS; Sercon 20/20). Through the combustion of collagen, nitrogen (N_2) and carbon dioxide (CO_2) were liberated. After the removal of water via the use of a chemical trap, these two gases were separated in a GC column packed with Carbosieve TM (Supelco G60/80 mesh; Bellefonte, Pennsylvania, USA) packing medium. During the process, helium (He) was used as a carrier gas and N_2 and CO_2 were sequentially analyzed on the IRMS for each sample. The calculations of δ^{13}C and δ^{15}N were performed relative to the results of an alanine standard and isotopic ratios are reported as delta per mil relative to the V-PDB and AIR international standards for carbon and nitrogen respectively (Coplen 1994). Details of this process can be found in Brock et al. (2010).

Eighteen well-preserved shells were prepared for carbonate δ^{13}C and δ^{18}O analyses. The last visible growth bands of the shells, comprising several annual growth increments and thus reflecting several seasons, were sampled, homogenized using a mortar and pestle and the carbonate sample analyzed at the Stable Isotope Facility of the University of California, Davis (SIF UCDavis) using a GasBench II system interfaced to a Delta V Plus IRMS (Thermo Scientific, Bremen, Germany). Approximately 0.3 mg of powdered sample was placed into vials and loaded into an autosampler rack (at 70ºC). Next, the capped vials were flushed/filled with helium using a CTC PAL autosampler device. Several drops of phosphoric acid (H_3PO_4) (103%) were then manually injected into each vial with the aid of a syringe to release CO_2. The vials were returned to the autosampler rack to equilibrate for 24 hr at 30°C. A Thermo Fisher Scientific Gas-Bench II device connected to a Thermo Fisher Scientific Delta V Plus gas-isotope ratio mass spectrometer was used to analyze the sample CO_2. Provisional δ values for the sample peak were acquired through the measurement of a pure CO_2 reference gas. These values were then corrected for changes in linearity and instrumental drift in order to yield accurate δ^{13}C and δ^{18}O for reference materials. The data were calibrated on the V-PDB scale using NBS 18 (–5.01‰, –23.01‰, for δ^{13}C and δ^{18}O respectively), NBS 19 (1.95‰, –2.20‰), and LSVEC (–46.60‰, –26.70‰).

Radiocarbon Dating

Carbonate: At the Radiocarbon Laboratory of the Universidade Federal Fluminense (LAC-UFF), carbonate pre-treatment follows the standard protocols for the preparation of inorganic samples (Oliveira et al. 2021). The remains of organic tissues were removed manually with scalpels and washing with MilliQ water was not necessary. For each shell, the last visible growth band, comprising several growth increments and thus reflecting several seasons, was sampled (~40 mg) and etched overnight with 0.8 mL of hydrochloric acid (HCl) 0.5M at 90ºC to remove the external layer (~50% of the sample). After the chemical pre-treatment, vials containing the samples were sealed with rubber septa and evacuated (<10 mTorr) in a vacuum line. Finally, 1mL of H_3PO_4 (85%) was inserted into each vial with the help of a syringe. The samples were left to react overnight at room temperature and the acid hydrolysis of $CaCO_3$ generated CO_2. The CO_2 obtained in the previous step was inserted into the vacuum line for purification. This process started with the use of a cryogenic trap of ethanol and dry ice (–78°C) to freeze the water present in the sample. CO_2 was then frozen with liquid nitrogen (–196°C) whilst other gases were discarded by

pumping. Next, CO_2 was transferred to a previously prepared graphitization tube, which consists of a small tube containing iron (Fe) inside a larger tube containing zinc (Zn) and titanium hydride (TiH_2). The graphitization tube was sealed with a torch and taken to the oven (7 hr at 550ºC) for the reduction of CO_2 to graphite (Xu et al. 2007; Macario et al. 2015a, 2017). The mixture of graphite and Fe, formed inside the inner reaction tube, was pressed in small aluminium cathodes. At the LAC-UFF, samples are measured in a 250 kV Single Stage Accelerator Mass Spectrometry (SSAMS) system produced by the National Electrostatics Corporation (NEC). This compact AMS, dedicated to the measurement of carbon isotopes, is the same system used at the Australian National University (ANU) [14]C Laboratory (Fallon et al. 2010), where some of the samples (graphite) were sent for measurement.

Bone: Bone samples were subjected to two different treatments at the ORAU. Samples coded AF underwent an acid-base-acid (ABA) treatment with 0.5M HCl (~4 rinses for over 18 hr), 0.1M sodium hydroxide (NaOH) (30 min) and 0.5M HCl (1 hr). Rinses with MilliQ water were performed between each step. The ABA treatment was followed by the gelatinization of collagen using pH 3 solution at 75ºC for 20 hr (Longin 1971) and ultrafiltration (Brown et al. 1988). Details of these steps can be found in Brock et al. (2010). The sample coded AG underwent the AF treatment without the ultrafiltration step in order to increase the collagen yield. Nevertheless, since this parameter is an indicator of the bone suitability for dating (and indeed of its preservation state), the AG pretreatment is only recommended in some special cases (see Brock et al. 2010). In both cases (AF and AG), the collagen samples were weighed into clean tin capsules. The tins containing purified collagen were taken to a collection system where they were combusted in an elemental analyzer (e.g., a Carlo-ERBA NA 2000). Hydrogen gas was added to the sample CO_2 and the mixture was collected and transferred to a specially designed rig containing Fe catalyst (Bronk Ramsey and Hedges 1997). The rig valve was then closed, and the reactor taken to the oven (6 hr at 560ºC). The final pressure in the reactors was measured to check for the completeness of the reaction. After that, the mixture of graphite and Fe was finally pressed in an aluminium cathode and taken to the ion source of a 2 MV accelerator system, produced by High Voltage Engineering Europa (HVEE), for measurement.

Charcoal: At the LAC-UFF, charcoal samples underwent an ABA treatment (Oliveira et al. 2021). This consisted of a wash with HCl 1.0M (2 hr at 90ºC), a wash with NaOH 1.0M (1 hr at 90ºC) and a second wash with HCl 1.0M (2 hr at 90ºC), performed in this order. In each step, the washes were repeated until the solution became clear and, after the final wash of each step, samples were rinsed with MilliQ water. The ABA treatment was carried out in order to remove contaminants such as carbonates and organic acids. The second acid step is necessary for the removal of atmospheric CO_2 contamination that may be introduced during the base step (Goh and Molloy 1972). After the chemical treatment, samples were dried and placed into previously prepared combustion tubes that were later evacuated and taken to a muffle furnace (3 hr at 900ºC). During this combustion step, the samples were converted to CO_2. Graphitization happened in the same way as for the shell samples.

MRE Determination
In order to ensure sample contemporaneity and take into account the overall variability in ΔR, Russell et al. (2011) propose a multipair approach. Following their method, several marine and terrestrial samples are selected for the ΔR calculation and every possible pairing is used. In the present study, for the calculation of ΔR values we have used the OxCal v4.2.4 calibration

software (Bronk Ramsey 2009), which has been shown to yield results equivalent to those obtained by the use of the multipair approach (Macario et al. 2015b). Charcoal ages were calibrated with the SHCal20 curve (Hogg et al. 2020) and shell ages were calibrated with the Marine20 curve (Heaton et al. 2020). By including the terrestrial and marine ages of each group of samples in the same phase and leaving ΔR undetermined (within the interval from -600 to 600 ^{14}C years), it was possible to evaluate the magnitude of the offset that would result in coeval samples (Bronk Ramsey 2013). The following models were employed in the present study (the codes can be found in the Supplementary Material):

Model 1: Considering that the burials can be from different time periods but the samples associated with a single burial are coeval, this model assumes an independent ΔR value for each burial (phase) (see Macario et al. 2015b).

Model 2: This follows the same premises of the first model but assuming a ΔR value that is roughly time-independent during the occupational period of the site, similar to the method employed by Macario et al. (2016).

Model 3: This approach considers all samples as part of the same occupational period (a single phase for all samples), which enhances the statistics of the model (Macario et al. 2015b).

Model 4: This is a single phase model for the derivation of a R value, similar to the one used by Milheira et al. (2017) for the study of the earthen mounds in Southern Brazil, for the whole set of samples.

Modeling Human Diet at Cabeçuda

The relative contribution of different food sources to human diet at Cabeçuda was calculated using a Bayesian mixing model in FRUITS 2.1.1 (Fernandes et al. 2014). In order to simplify the model, only the most important components of the diet (i.e., fish, terrestrial mammals and C_3 plants), based on the archaeological evidence, were included in the model input. The $\delta^{13}C$ and $\delta^{15}N$ values of 17 fish specimens from Southern Brazil, reported in Colonese et al. (2014), were averaged to yield -11.4 ± 1.4‰ and $+13.5 \pm 2.0$‰, respectively. These samples consisted of archaeological and modern marine-brackish species from the Santa Catarina coast. Colonese et al. (2014) also report isotopic data for 14 archaeological samples of herbivorous and omnivorous specimens from the Southeastern Atlantic Forest of Brazil. The average $\delta^{13}C$ and $\delta^{15}N$ values of these terrestrial animals are -22 ± 1.2‰ and $+8.4 \pm 1.7$‰, respectively. Finally, the plant isotopic data used in the model were obtained from Galetti et al. (2016), who analyzed 48 samples [modern fruits (n = 30); roots (n = 5) and palm-heart (n = 13)] from the Southeastern Atlantic Forest, obtaining average $\delta^{13}C$ and $\delta^{15}N$ values of -29.2 ± 3.0‰ and $+1.1 \pm 2.0$‰, respectively. Modern plant samples had their $\delta^{13}C$ values corrected for the Suess Effect using a value of $+2$‰ (Hellevang and Aagaard 2015).

The isotopic values of the food sources refer to the bulk of each food source and offsets need to be applied for the derivation of the isotopic signature of their macronutrient fractions (protein, carbohydrate, and lipids). Following Fernandes et al. (2015) and Fernandes (2016), the offsets employed in the model were -2‰ ($\Delta^{13}C_{protein-collagen}$), -8‰ ($\Delta^{13}C_{lipids-collagen}$) and $+2$‰ ($\Delta^{15}N_{protein-collagen}$) for terrestrial mammals, -1‰ ($\Delta^{13}C_{protein-collagen}$), -7‰ ($\Delta^{13}C_{lipids-collagen}$) and $+2$‰ ($\Delta^{15}N_{protein-collagen}$) for fish and -2‰ ($\Delta^{13}C_{bulk-protein}$) and $+0.5$‰ ($\Delta^{13}C_{bulk-lipids}$), and $\delta^{15}N_{protein} = \delta^{15}N_{bulk}$ for plants. An uncertainty of 1‰ was applied to all of these offsets. While the nitrogen content of collagen is assumed to be exclusively derived from proteins, carbon can be obtained

from carbohydrates or lipids via the *de novo* synthesis of non-essential amino acids (Jim et al. 2006; Fernandes et al. 2012; Webb et al. 2017). Hence, we have assumed that protein and energy (representing lipids and carbohydrates) contribute with 74 ± 4% and 26 ± 4% of carbon to bulk collagen, respectively (Fernandes et al. 2012). The Bayesian analysis of the isotopic data of the individuals of Cabeçuda (Fernandes 2016) was performed with a model using $\delta^{13}C$ and $\delta^{15}N$ diet-to-collagen offsets of +5 ± 0.5‰ (Fernandes et al. 2012). The model assumed a range of protein intake of >5% and <45% of the total calories (Fernandes et al. 2014).

RESULTS AND DISCUSSION

Table 1 presents the results of the analyses of the charcoal and shell samples collected at Cabeçuda.

The XRD results for the shells are presented in the Supplementary Material. Although the results show the presence of an amorphous phase that may contain organic carbon, this would not be converted to CO_2 during the acid hydrolysis of the sample and thus does not constitute contamination. Indeed, the XRD results point to a crystalline structure that is primarily aragonite, which means that aragonite to calcite recrystallization is not an issue for the archaeological shells used in this study. Similar conclusions were obtained by Colonese et al. (2014) on shells from this site. In any case, the etching procedure performed for the shells has been shown to be a valid method to eliminate any possible secondary calcite (e.g., Macario et al. 2017).

The $\delta^{13}C$ and $\delta^{18}O$ values for the Cabeçuda shells are in the range from +0.96 to +1.81‰ and from –1.35 to –0.31‰, respectively. These values are within the range found by Casati (2019) for several *Anomalocardia* shells from Cabeçuda and nearby sites. They are also broadly consistent with the modeled present-day values for the South Atlantic ocean (see Gruber et al. 1999; LeGrande and Schmidt 2006; Tagliabue and Bopp 2008) and these two variables show no correlation in the set of samples analyzed in the present study (Figure 3a). The negative $\delta^{18}O$ signal points to the influence of higher temperatures or freshwater input by the regional rivers. In this context, the positive $\delta^{13}C$ values could be a result of enhanced primary production through upwelling as proposed by recent studies, and in such case would also reflect inputs from oceanic waters (e.g., Toniolo et al. 2020). Figure 3b shows that the $\delta^{18}O$ values remain broadly constant. The $\delta^{13}C$ values, on the other hand, seem to decrease with time (Figure 3c). This is also consistent with data presented by Casati (2019) and may be due to a lower marine influence in this period, possibly related to decreasing sea-level. According to Casati (2019), other possible influencing factors for this trend include the progressive closure of the connections between the lagoon and the sea due to siltation (Giannini et al. 2010), increasing rainfall leading to enhanced fluvial input in the region (e.g., Cruz et al. 2007; Bernal et al. 2016) and the progradation of the Tubarão river delta increasing its influence in the lagoon (Nascimento 2010). It is here assumed that molluscs were collected from areas surrounding the site, and thus their $\delta^{13}C$ and $\delta^{18}O$ values would reflect local environmental conditions. However, given the volume and the long-term use of the site such an assumption may be arguable. Previous studies have shown that shellfish exploitation by coastal foragers may occur at several distances from the depositional sites (Andrus and Thompson 2012). Therefore, collections in areas exposed to distinct degrees of freshwater and sea water circulation could explain some of the variability observed in shell $\delta^{13}C$ and $\delta^{18}O$ values, but further

Table 1 Anthracological and isotopic results, including ^{14}C-AMS, for archaeological samples from the shell mound Sambaqui de Cabeçuda. The uncertainties for the δ^{13}C and δ^{18}O values are 0.10 and 0.20‰, respectively.

Site	LAC-UFF code	Material	Species/family	Burial	^{14}C age ± 1σ (^{14}C yr BP)	$\delta^{13}C_{VPDB}$ (‰)	$\delta^{18}O_{VPDB}$ (‰)
Cabeçuda	180303*	Shell	*Anomalocardia flexuosa*	1	3725 ± 30	1.44	–0.78
Cabeçuda	180304*	Shell	*Anomalocardia flexuosa*	1	3750 ± 35	1.07	–1.10
Cabeçuda	180305*	Shell	*Anomalocardia flexuosa*	1	3705 ± 35	1.76	–0.77
Cabeçuda	180200	Charcoal	Sapotaceae	1	3868 ± 50	—	—
Cabeçuda	190364	Charcoal	Rutaceae	1	3431 ± 39	—	—
Cabeçuda	190365	Charcoal	Rutaceae	1	3593 ± 38	—	—
Cabeçuda	180306*	Shell	*Anomalocardia flexuosa*	3	3740 ± 35	1.07	–1.34
Cabeçuda	180307*	Shell	*Anomalocardia flexuosa*	3	3735 ± 30	1.26	–1.35
Cabeçuda	180308*	Shell	*Anomalocardia flexuosa*	3	3735 ± 30	1.79	–0.83
Cabeçuda	180201	Charcoal	Bark (undetermined)	3	3859 ± 50	—	—
Cabeçuda	190366	Charcoal	Sapindaceae	3	3451 ± 38	—	—
Cabeçuda	180309*	Shell	*Anomalocardia flexuosa*	5	3795 ± 35	1.37	–0.99
Cabeçuda	180310*	Shell	*Anomalocardia flexuosa*	5	3835 ± 30	1.46	–1.08
Cabeçuda	180268*	Shell	*Anomalocardia flexuosa*	5	3675 ± 25	1.04	–0.85
Cabeçuda	180202	Charcoal	Myrtaceae	5	4229 ± 54	—	—
Cabeçuda	190367	Charcoal	Myrtaceae	5	3529 ± 37	—	—
Cabeçuda	190368	Charcoal	Leguminosae	5	3604 ± 38	—	—
Cabeçuda	180311*	Shell	*Anomalocardia flexuosa*	6	4035 ± 40	1.62	–0.31
Cabeçuda	180312*	Shell	*Anomalocardia flexuosa*	6	3805 ± 35	1.25	–1.12
Cabeçuda	180286	Shell	*Anomalocardia flexuosa*	6	3847 ± 41	0.96	–1.05
Cabeçuda	180203	Charcoal	Nut	6	3647 ± 52	—	—
Cabeçuda	190369	Charcoal	Sapotaceae	6	3858 ± 44	—	—
Cabeçuda	190370	Charcoal	Leguminosae	6	3846 ± 42	—	—
Cabeçuda	180272*	Shell	*Anomalocardia flexuosa*	7	3995 ± 35	1.79	–1.11
Cabeçuda	180313*	Shell	*Anomalocardia flexuosa*	7	3935 ± 35	1.50	–0.70
Cabeçuda	180314*	Shell	*Anomalocardia flexuosa*	7	3985 ± 30	1.54	–1.34
Cabeçuda	180253*	Charcoal	Twig (undetermined)	7	3760 ± 35	—	—
Cabeçuda	190371	Charcoal	Myrtaceae	7	3988 ± 40	—	—

Table 1 (*Continued*)

Site	LAC-UFF code	Material	Species/family	Burial	^{14}C age ± 1σ (^{14}C yr BP)	$\delta^{13}C_{VPDB}$ (‰)	$\delta^{18}O_{VPDB}$ (‰)
Cabeçuda	190372	Charcoal	Sapotaceae	7	3832 ± 44	—	—
Cabeçuda	180315	Shell	*Anomalocardia flexuosa*	13	4085 ± 35	1.76	–0.76
Cabeçuda	180316	Shell	*Anomalocardia flexuosa*	13	3925 ± 35	1.41	–1.02
Cabeçuda	180317	Shell	*Anomalocardia flexuosa*	13	4060 ± 30	1.81	–0.96
Cabeçuda	180204	Charcoal	Bark (undetermined)	13	3865 ± 50	—	—
Cabeçuda	220026	Charcoal	Rutaceae	13	3660 ± 30	—	—

*These samples were measured at the ANU ^{14}C Laboratory.
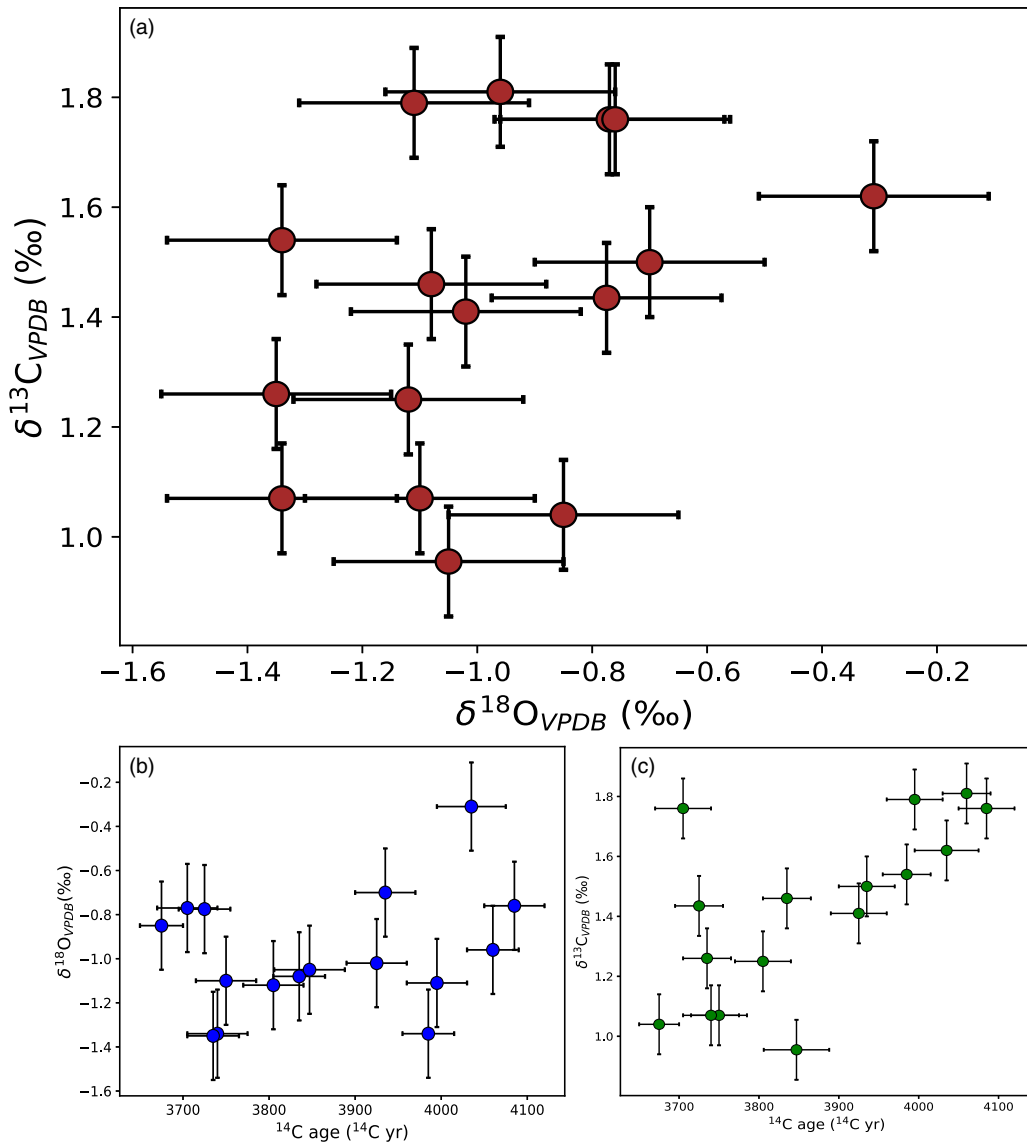
Figure 3   (a) Stable isotopes (δ¹⁸O and δ¹³C) results for the archaeological shells. (b) δ¹⁸O and (c) δ¹³C results versus time for the archaeological shells.

studies are required to validate this hypothesis. Moreover, it is important to notice that in Figure 3 the radiocarbon ages are not calibrated.

Deriving a ΔR Value for the Sambaqui de Cabeçuda

Highly negative ΔR values were obtained for Cabeçuda. Model 1 yields ΔR values that range from –316 ± 205 to –160 ± 143 ^{14}C yr (Figure 4). However, although this model is ideal for assessing temporal variations, our small sample set is a drawback. Due to the limited number of samples in each phase, any outlier can lead to inaccurate results for the ΔR. For example,
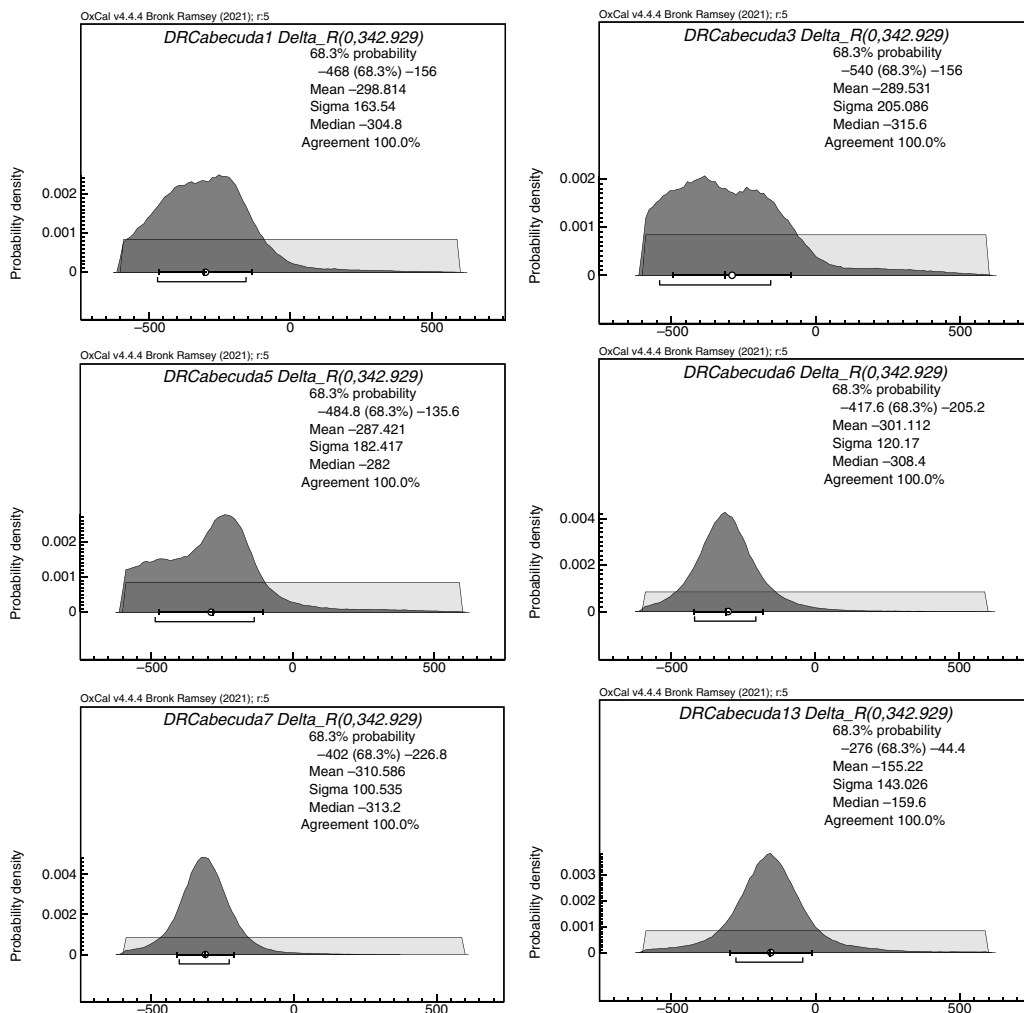
Figure 4   Individual ∆R values obtained for each Cabeçuda burial studied (model 1).

outlier analysis included in model 1 (Bronk Ramsey 2009) revealed that sample 180202 is an outlier at 41% probability (see Supplementary Material). In order to bypass this obstacle and given that the results of model 1 do not hint at a considerable temporal variation of ∆R, model 2 employs separate phases but all the dates are used to achieve a common ∆R for the site.

The approach of model 2 yielded a ∆R of –271 ± 52 ^{14}C yr (Figure 5a). By having a closer look at this model (see Supplementary Material), it is possible to note that burial 5 is problematic, with the charcoal (sample 180202), which is identified as an outlier (58%), being older than the shells. A possible reason for this inconsistency is the remobilization of the charcoal fragment, meaning that it would not be originally associated with the burial. This means that more charcoal samples derived from this burial need to be measured for this research. Finally, model 3 maximizes the statistics of the ∆R derivation by considering the whole set of dates within a single phase. By employing this model, a ∆R value of –275 ± 58 ^{14}C yr was derived for the site (Figure 5b).
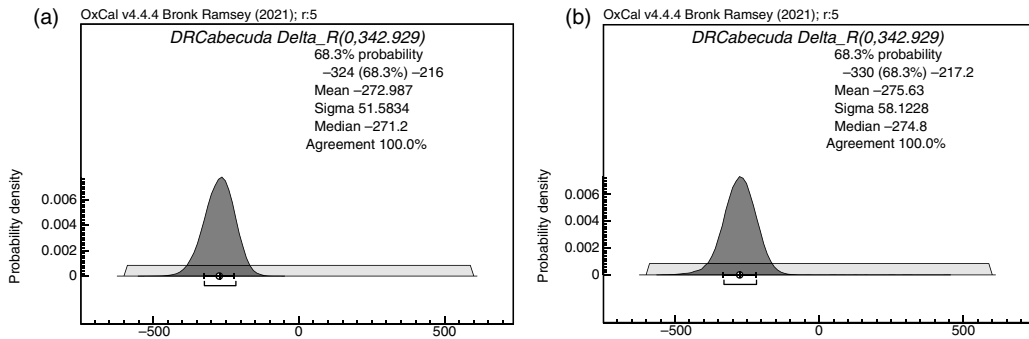
Figure 5   A common ∆R value obtained for all the Cabeçuda burials studied using a model with (a) different phases (model 2) and (b) a single phase (model 3) for the Cabeçuda burials.
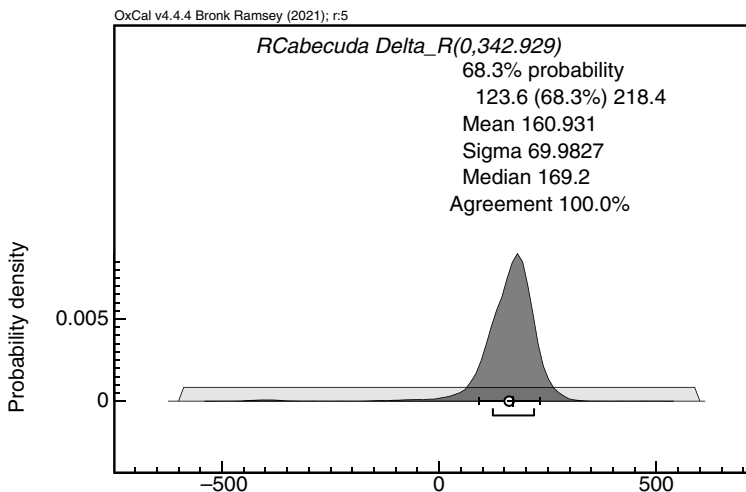

Figure 6   Single R value obtained considering a single phase for the Cabeçuda burials (model 4).

Model 3 assumes that all samples are coeval, but the outlier model shows that sample 180202 is remarkably older (see Supplementary Material). Moreover, samples 190364 and 190371 are also identified as outliers at different probabilities. If the charcoal dates were reliable, the highly negative ∆R results obtained in the present study would indicate that aquatic samples from the LLS could be accurately calibrated by the use of the SHCal20 atmospheric curve and the R offset (instead of Marine20 and ∆R). Model 4 yields the value of R = 169 ± 70 ^{14}C yr (Figure 6). A drawback of this approach is that marine ^{14}C ages calibrated with atmospheric curves yield calibrated age distributions that present the oscillations characteristic of the atmospheric reservoir.

The ∆R values derived in the present study are very negative and some probability distributions in Figure 4 are truncated even within the –600 to 600 ^{14}C yr range used in the model. The samples identified as outliers in model 3 (180202, 190364, and 190371) are charcoal pieces associated with burials 1, 5, and 7, and could have been remobilized. Therefore, it is important to acknowledge the possibility of these samples being unsuitable
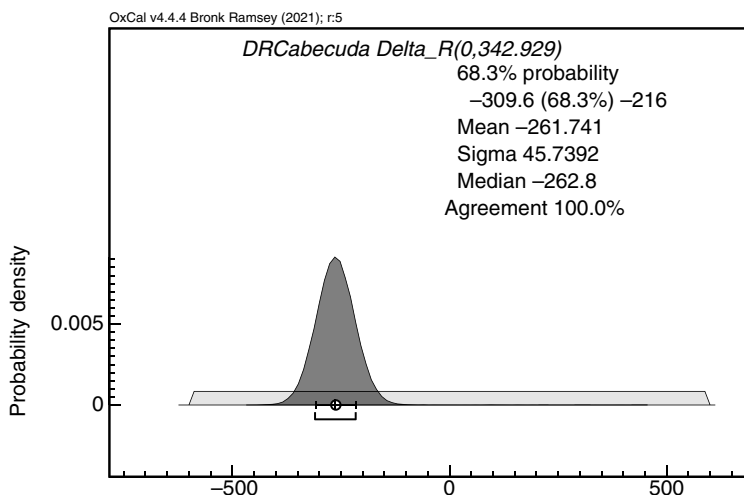
Figure 7   Single ΔR value obtained considering a single phase for the Cabeçuda burials. Outliers (samples 180202, 190364, and 190371) were excluded from this analysis.

for MRE determinations (i.e., not coeval). Taking this into consideration and excluding these samples from the third model presented here, a ΔR of –263 ± 46 ^{14}C yr is obtained (Figure 7). This is the most reliable of all the approaches so far presented. Despite the very low chances in the restinga environment, charcoal samples 180202, 190364, and 190371 could possibly be affected by the old-wood effect. Therefore, given that the shells do not present recrystallization, by excluding these samples from the ΔR determination the chances of remobilization or an old-wood effect affecting the result were also further minimized. The ΔR value of –263 ± 46 ^{14}C yr is therefore the one to be used for Cabeçuda until more samples are measured for the improvement of the statistics.

These results are highly negative, similarly to what is observed in the present day ΔR values of –114 ± 25 and –244 ± 53 ^{14}C yr derived for the coast of Santa Catarina (Alves et al. 2020). In Southern Brazil, only two other archaeological sites were studied for MRE quantification: the earthen mound complex in Patos Lagoon (R = 63 ± 53 ^{14}C yr; Milheira et al. 2017) and the Sambaqui de Jabuticabeira (ΔR = –205 ± 80 ^{14}C yr), both showing results consistent with our findings for Cabeçuda. The latter value was re-calculated using Marine20 and the same approach in model 2 from the data presented in Eastoe et al. (2002). To understand our results, it is important to consider the environmental setting of the LLS. This lagoonal system was formed when the post-glacial rise in sea-level drowned pre-existing incised valleys during the Mid Holocene (Amaral et al. 2012), and since then, it presents an increasingly restricted connection to the sea, which enhances the effect of terrestrial carbon input by the discharge of major rivers in this reservoir. This phenomenon is even more significant when one considers that the seawater entering the lagoon may be influenced by the plume of the La Plata River (Toniolo et al. 2020), which is the second largest river in South America (e.g., Piola et al. 2000, 2005; Piola and Romero 2004; Pimenta et al. 2005). In addition, the shallow depths of the lagoons suggest that these are well-mixed reservoirs that could be in isotopic equilibrium with atmospheric CO_2. Although Colonese et al. (2017), who analyzed stable isotopes of carbon and oxygen in archaeological samples from Cabeçuda, report a higher marine influence in the system at 3 ka cal BP when compared to

Table 2   Results for the bone samples analyzed in the present study.

Site	Material	Identification	Treatment	Sample	Burial	OxA code	^{14}C age ± 1σ (^{14}C yr BP)	$\delta^{13}C_{VPDB}$ (‰)	$\delta^{15}N_{AIR}$ (‰)	C:N
Cabeçuda	Bone	Human (pelvis)	AF	43,230	1	35,552	3762 ± 28	–10.5	18.7	3.2
Cabeçuda	Bone	Human (femur)	AG	43,231	3	X-2722-37	3761 ± 31	–9.5	18.5	3.3
Cabeçuda	Bone	Human (torax)	AF	43,232	5	35,553	3768 ± 29	–9.8	17.7	3.2
Cabeçuda	Bone	Human	AF	43,233	6	35,554	3930 ± 31	–10.5	19.2	3.2
Cabeçuda	Bone	Human	AF	43,234	7	—	—	—	—	—
Cabeçuda	Bone	Human (torax)	AF	43,235	13	36,750	3539 ± 27	–12.5	18	3.5

the present-day conditions, the ΔR value derived here shows continental influence. The analyses of samples from different archaeological layers at Cabeçuda would allow for the assessment of the MRE temporal variation but, unfortunately, this was not possible due to the poor preservation of the site. Since the Brazilian sambaquis are often found near coastal lagoons due to the productivity of these environments, negative ΔR values are not uncommon (Macario et al. 2018) and the same approach may suit other settlements.

Diet Assessment and Chronology in the Sambaqui de Cabeçuda

Table 2 presents the results for the bone samples. With the exception of burial 7, collagen was extracted from all human bones. The collagen C:N atomic weight ratios were within the interval (2.9–3.5) characteristic of intact collagen (van Klinken 1999). The radiocarbon ages of these samples fall within the range 4000–3500 yr BP, in agreement with previous results for other samples derived from the same excavation. The mean $\delta^{13}C$ and $\delta^{15}N$ values for the five individuals were –10.6 ± 1.4‰ and +18.4 ± 0.5‰ respectively, indicating diets with high intake of marine proteins.

According to the model parameters and assumptions, marine fish and C3 plants were the main sources of dietary calories to humans of Cabeçuda (see Supplementary Material), which is in agreement with zooarchaeological data obtained from the sambaqui deposit (Klokler 2016). The model outputs indicate that for all humans most of the carbon atoms in collagen derived from fish, with relative contributions ranging from 74 ± 4% (burial 13) to 82 ± 4% (burial 3).

A highly marine diet bears important consequences to the calibration of radiocarbon ages obtained from human remains (see Pezo-Lanfranco et al. 2018; Fossile et al. 2019; Toso et al. 2021). In the specific case of Cabeçuda, the ΔR value calculated in this work can be applied for correcting the ^{14}C ages obtained from the individuals. Based on the contributions of each of the most significant food sources to the diet of the Cabeçuda builders, as estimated by Bayesian modeling in the previous section, the bone samples analyzed in this paper were calibrated with mixed calibration curves (using the respective percentual contribution of marine carbon to collagen carbon) and the ΔR derived here (–263 ± 46 ^{14}C yr) (Figure 8).

Using a phase model for the Cabeçuda bones it is possible to estimate a period between approximately 4200 and 3600 cal BP (Figure 9) within the occupation. However, it is important to emphasize that this is not representative for the whole site since Cabeçuda is much larger than the studied burials.

CONCLUSIONS

The Sambaqui de Cabeçuda is an impressive Brazilian coastal shell mound, which holds important paleoenvironmental and archaeological information. Here, we employed an interdisciplinary approach involving stable isotopes, carbonate geochemistry, radiocarbon dates on shell, bone and charcoal remains from the site, as well as Bayesian models to derive (1) an accurate MRE offset for the region, (2) the age of human burials, and (3) the diet of the inhumated individuals. Our model outputs reveal that the local MRE was highly negative (–263 ± 46 ^{14}C yr) and this must be considered when calibrating local conventional radiocarbon dates derived from marine organisms (e.g., shells, fish) and
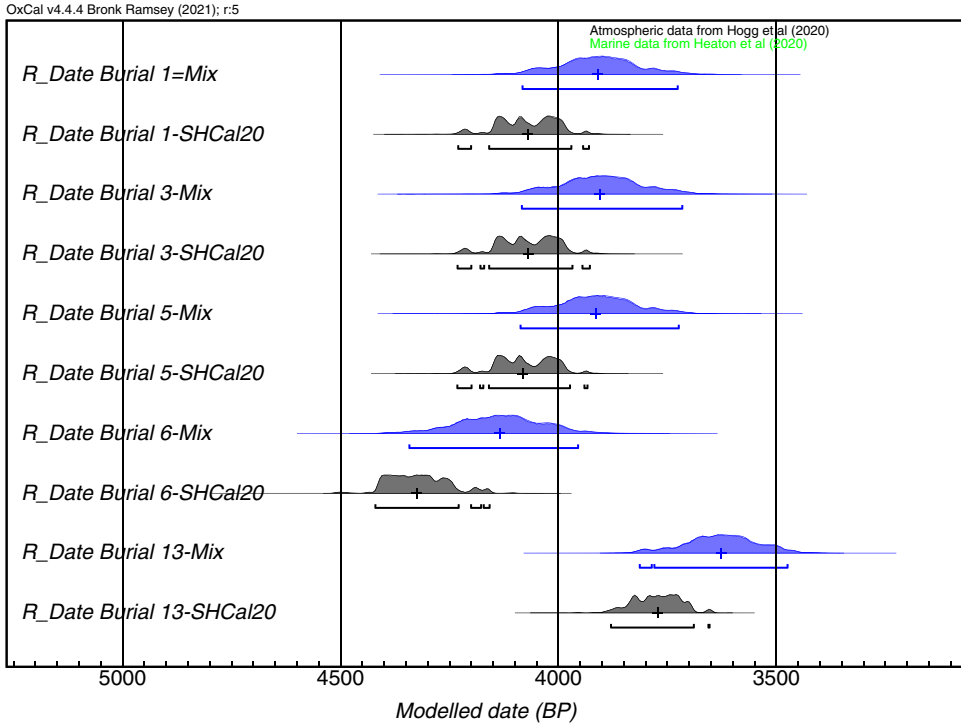
OxCal v4.4.4 Bronk Ramsey (2021); r:5

Atmospheric data from Hogg et al (2020)
Marine data from Heaton et al (2020)

R_Date Burial 1=Mix

R_Date Burial 1-SHCal20

R_Date Burial 3-Mix

R_Date Burial 3-SHCal20

R_Date Burial 5-Mix

R_Date Burial 5-SHCal20

R_Date Burial 6-Mix

R_Date Burial 6-SHCal20

R_Date Burial 13-Mix

R_Date Burial 13-SHCal20

5000   4500   4000   3500

Modelled date (BP)

Figure 8   Comparison between the calibration of the ages obtained from the humans of Cabeçuda using a SHCal20/ Marine20 mixed curve (purple) and only the SHCal20 curve (black).

OxCal v4.4.4 Bronk Ramsey (2021); r:5

Sequence

Boundary Start 1

Phase 1

Boundary End 1

7000   6000   5000   4000   3000   2000
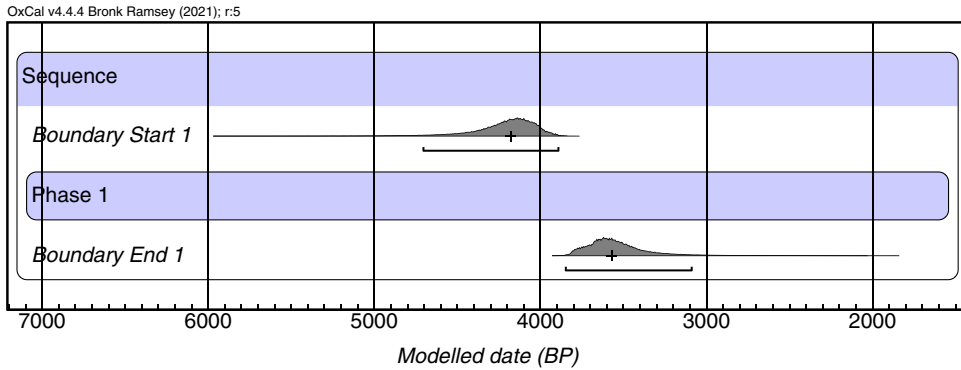
Modelled date (BP)

Figure 9   Boundaries of a phase model for the Cabeçuda bones.

human remains (collagen, apatite) whose dietary proteins were dominated by marine resources. This was the case for all the human individuals analyzed in this study. Stable isotope and Bayesian Isotope Mixing Models pointed to dietary regimes with high intakes of marine proteins. By quantifying the MRE, a correction factor for the radiocarbon dates (ΔR) enabled us to accurately model their ages between ca. 4200 and 3600 cal BP. Based on our

results, we argue that the following steps should be taken for reliable MRE studies to be performed in Brazilian shell mounds:

1. **Stratigraphic control:** MRE studies rest on the assumption of contemporaneity between terrestrial and marine materials. Previous studies have outlined measures to guarantee that the samples are coeval and thus ensure the suitability of archaeological contexts for MRE calculation. Whenever possible, archaeologists sampling for this purpose should follow these guidelines.

2. **Post-depositional effects and inbuilt ages must be taken into account:** Each type of material introduce biases in radiocarbon dating. These should be anticipated by the researcher and analyzed beforehand with the aim of minimizing any interferences in the accuracy of the derived MRE offset.

3. **Multiple possibilities of Bayesian modeling:** For the derivation of MRE offsets, different Bayesian models should be tested. This will allow for the identification of the most accurate priors to be used with the set of ^{14}C dates under analysis. In the present study, we have employed four different models and discussed their results alongside their advantages and limitations.

4. **Human diet should be assessed prior to radiocarbon dating bones:** Human bone is often radiocarbon dated to derive direct and secure ages of burial events. However, human bones can be also affected by the MRE in populations with dietary regimes based on marine organisms. It is of paramount importance to evaluate individual diets using stable isotopes prior radiocarbon dating.

SUPPLEMENTARY MATERIAL

To view supplementary material for this article, please visit https://doi.org/10.1017/RDC.2022.75

ACKNOWLEDGMENTS

REFERENCES

Abbott R. 1974. American seashells; the marine molluska of the Atlantic and Pacific coasts of North America. New York: Van Nostrand Reinhold.

Aitken M. 1900. Science-based dating in archaeology. London: Routledge.

Albero MC, Angiolini FE, Piana E. 1986. Discordant ages related to reservoir effect of associated archaeologic remains from the tunel site, beagle channel, Argentine Republic. Radiocarbon 28(2): 748–753.

Als-Nielsen J, McMorrow D. 2011. Elements of modern X-ray physics. Jon Wiley & Sons. 2nd edition.

Alves EQ, Macario KD, Spotorno-Oliveira P, Oliveira FM, Muniz MC, Fallon S, et al. 2020. Nineteenth century expeditions and the radiocarbon marine reservoir effect on the Brazilian coast. Geochimica et Cosmochimica Acta.

Alves E, Macario K, Ascough P, Bronk Ramsey C. 2018. The worldwide marine radiocarbon reservoir effect: definitions, mechanisms, and prospects. Reviews of Geophysics 56:1–28.

Amaral PGC, Fonseca Giannini PC, Sylvestre F, Ruiz Pessenda LC. 2012. Paleoenvironmental reconstruction of a Late Quaternary lagoon system in southern Brazil (Jaguaruna region, Santa Catarina state) based on multi-proxy analysis. Journal of Quaternary Science 27(2):181–191.

Ambrose SH. 1986. Stable carbon and nitrogen isotope analysis of human and animal diet in Africa. Journal of Human Evolution 15(8): 707–731.

Anderson A. 1991. The chronology of colonization in New Zealand. Antiquity 65(249):767–795.

Andrus CFT, Thompson VD. 2012. Determining the habitats of mollusk collection at the Sapelo Island shell ring complex, Georgia, USA using oxygen isotope sclerochronology. Journal of Archaeological Science 39(2):215–228.

Angulo RJ, Giannini PCF, Suguio K, Pessenda LCR. 1999. Relative sea-level changes in the last 5500 years in southern Brazil (Laguna – Imbituba region, Santa Catarina State) based on vermetid ^{14}C ages. Marine Geology 159:323–339.

Angulo RJ, Lessa GC, de Souza M. 2006. A critical review of mid- to late-Holocene sea-level fluctuations on the eastern Brazilian coastline. Quaternary Science Reviews 25:486–506.

Arneborg J, Heinemeier J, Lynnerup N, Nielsen H, Rud N, Sveinbjornsdottir A. 1999. Change of diet of the Greenland Vikings determined from stable carbon analysis and ^{14}C dating of their bones. Radiocarbon 41(2):157–168.

Ascough P, Cook G, Dugmore A. 2005. Methodological approaches to determining the marine radiocarbon reservoir effect. Progress in Physical Geography: Earth and Environment 29(4):532–547.

Barletta M, Lima ARA, Dantas DV, Oliveira IM, Neto JR, Fernandes CAF, Farias EGG, Filho JLR, Costa MF. 2017. How can accurate landing stats help in designing better fisheries and environmental management for Western Atlantic estuaries? In: Finkl CW, Makowski C,

editors. Coastal wetlands: alteration and remediation. Springer. p. 631–703.

Bayliss A. 2009. Rolling out revolution: using radiocarbon dating in archaeology. Radiocarbon 51(1):123–147.

Beavan NR, Sparks RJ. 1998. Factors influencing ^{14}C ages of the pacific rat *Rattus exulans*. Radiocarbon 40(2):601–613.

Beavan-Athfield NR, McFadgen BG, Sparks RJ. 2001. Environmental influences on dietary carbon and ^{14}C ages in modern rats and other species. Radiocarbon 43(1):7–14.

Bernal JP, Cruz FW, Stríkis NM, Wang X, Deininger M, Catunda MCA, et al. 2016. High-resolution Holocene South American monsoon history recorded by a speleothem from Botuverá Cave, Brazil. Earth and Planetary Science Letters 450:186–196.

Boehs G, Magalhães ARM. 2004. Simbiontes associados com Anomalocardia brasiliana (Gmelin) (*Mollusca, Bivalvia, Veneridae*) na Ilha de Santa Catarina e região continental adjacente, Santa Catarina, Brasil.

Brock F, Higham T, Ditchfield P, Ramsey CB. 2010). Current pretreatment methods for AMS radiocarbon dating at the Oxford Radiocarbon Accelerator Unit (ORAU). Radiocarbon 52(1): 103–112.

Bronk Ramsey C. 2009. Bayesian analysis of radiocarbon dates. Radiocarbon 51(1):337–360.

Bronk Ramsey C. 2009b. Dealing with outliers and offsets in radiocarbon dating. Radiocarbon 51(3):1023–1045.

Bronk Ramsey C. 2013. Recent and planned developments of the Program OxCal. Radiocarbon 55(3–4):720–730.

Bronk Ramsey C, Hedges R. 1997. Hybrid ion sources: radiocarbon measurements from microgram to milligram. Nuclear Instruments and Methods in Physics Research Section B: Beam Interactions with Materials and Atoms 123(1–4):539–545.

Brown TA, Nelson DE, Vogel JS, Southon JR. 1988. Improved collagen extraction by modified Longin method. Radiocarbon 30(2):171–177.

Bruhns K. 1994. Ancient South America. Cambridge University Press.

Budowski G. 1965. Distribution of tropical American rain forest species in the light of successional processes. Turrialba 15(1):40–42

Byrne C, Dotte-Sarout E, Winton V. 2013. Charcoals as indicators of ancient tree and fuel strategies: an application of anthracology in the Australian Midwest. Australian Archaeology 77:94–106.

Casati R. 2019. O registro climático e ambiental das conchas de sambaquis e depósitos paleolagunares na costa centro-sul Catarinense [doctoral dissertation]. Universidade de São Paulo.

Chappell J, Polach H. 1972. Some effects of partial recrystallisation on ^{14}C dating Late Pleistocene corals and molluscs. Quaternary Research 252.

Chisholm B, Nelson DE, Schwarcz HP. 1982. Stable-carbon isotope ratios as a measure of marine versus terrestrial protein in ancient diets. Science 216:11131–11132.

Colonese AC, Collins M, Lucquin A, Eustace M, Hancock Y, Ponzoni RDAR, Mora A, Smith C, DeBlasis P, Figuti L, et al. 2014. Long-term resilience of late Holocene coastal subsistence system in southeastern South America. PLoS ONE 9(4):1–13.

Colonese C, Netto S, Francisco A, Deblasis P, Villagran XS, Ponzoni R, Hancock Y, Hausmann N, Farias D, Prendergast A, et al. 2017. Shell sclerochronology and stable isotopes of the bivalve *Anomalocardia flexuosa* (Linnaeus, 1767) from southern Brazil: Implications for environmental and archaeological studies. Palaeogeography, Palaeoclimatology, Palaeo-ecology 484:7–21.

Commendador A. 2014. Radiocarbon dating human skeletal material on Rapa Nui: Evaluating the effect of uncertainty in marine-derived carbon. Radiocarbon 56(1):277–294.

Cook GT, Ascough PL, Bonsall C, Hamilton WD, Russell N, Sayle KL, Scott EM, Bownes JM. 2015. Best practice methodology for ^{14}C calibration of marine and mixed terrestrial/marine samples. Quaternary Geochronology 27:164–171.

Coplen TB. 1994. Reporting of stable hydrogen, carbon, and oxygen isotopic abundances (Technical Report). Pure and Applied Chemistry 66(2):273–276.

Cruz Jr, FW, Burns SJ, Jercinovic M, Karmann I, Sharp WD, Vuille M. 2007. Evidence of rainfall variations in Southern Brazil from trace element ratios (Mg/Ca and Sr/Ca) in a Late Pleistocene stalagmite. Geochimica et Cosmochimica Acta 71(9):2250–2263.

DeBlasis P, Fish SK, Gaspar MD, Fish PR. 1998. Some references for the discussion of complexity among the Sambaqui moundbuilders from the southern shores of Brazil. Revista de Arqueologia Americana (15):75–105.

DeBlasis P, Kneip A, Scheel-Ybert R, Giannini PC, Gaspar MD. 2007. Sambaquis e Paisagem – Dinâmica natural e arqueologia regional no litoral do sul do Brasil. Arqueología Suramericana 3(1):29–61.

Deforce K, Boeren I, Adriaenssens S, Bastiaens J, De Keersmaeker L, Haneca K, Tys D, Vandekerkhove K. 2013. Selective woodland exploitation for charcoal production. A detailed analysis of charcoal kiln remains (ca. 1300–1900 AD) from Zoersel (northern Belgium). Journal of Archaeological Science 40(1):681–689.

de Souza R, Lima T, da Silva E. 2011. Conchas Marinhas de Sambaquis do Brasil. Technical Books.

Detienne P, Jacquet P. 1983. Atlas d'identification des bois de l'Amazonie et des regions voisines. Centre Technique Forestier Tropical, France.

Douka K, Hedges RM, Higham TG. 2010. Improved AMS ^{14}C dating of shell carbonates using high-precision X-Ray Diffraction and a Novel Density Separation Protocol (CarDS). Radiocarbon 52(2):735–751.

Emery-Barbier A, Thiébault S. 2005. Preliminary conclusions on the Late Glacial vegetation in south-west Anatolia (Turkey): the complementary nature of palynological and anthracological approaches. Journal of Archaeological Science 32(8):1232–1251.

Enmar R, Stein M, Bar-Matthews M, Sass, E, Katz, A, Lazar, B. 2000. Diagenesis in live corals from the Gulf of Aqaba. I. The effect on paleo-oceanography tracers. Geochimica et Cosmochimica Acta, 64(18):3123–3132.

Erlandson JONM, Kennett DJ, Ingram BL, Guthrie DA, Morris DONP, Tveskov MAT, West, GJ, Walker PL. 1996. An archaeological and paleontological chronology for Daisy Cave (CA-SMI-261), San Miguel Island, California. Radiocarbon 38(2):355–373.

Ervynck A. 2014. Dating human remains from the historical period in Belgium: diet changes and the impact of marine and freshwater reservoir effects. Radiocarbon 56(2):779–788.

Eastoe CJ, Fish S, Fish P, Gaspar MD, Long A. 2002. Reservoir corrections for marine samples from the south Atlantic coast, Santa Catarina State, Brazil. Radiocarbon 44(1):145–148.

Euba I, Allué E, Burjachs F. 2016. Wood uses at El Mirador Cave (Atapuerca, Burgos) based on anthracology and dendrology. Quaternary International 414:285–293.

Facorellis Y. 1998. Apparent ^{14}C ages of marine mollusk shells from a Greek Island: Calculation of the marine reservoir effect in the Aegean Sea. Radiocarbon 40(2):963–973.

Fallon SJ, Fifield LK, Chappell JM. 2010. The next chapter in radiocarbon dating at the Australian National University: status report on the s ingle stage AMS. Nuclear Instruments and Methods in Physics Research, Section B: Beam Interactions with Materials and Atoms 268(7–8):898–901.

Feigl F. 1958. Spot tests in inorganic analysis. Amsterdam: Elsevier.

Fernandes R. 2016. A Simple(r) model to predict the source of dietary carbon in individual consumers. Archaeometry 58(3):500–512.

Fernandes R, Grootes P, Nadeau MJ, Nehlich O. 2015. Quantitative diet reconstruction of a Neolithic population using a Bayesian mixing model (FRUITS): the case study of Ostorf (Germany). American Journal of Physical Anthropology 158(2):325–340.

Fernandes R, Millard AR, Brabec M, Nadeau MJ, Grootes P. 2014. Food reconstruction using isotopic transferred signals (FRUITS): a Bayesian model for diet reconstruction. PLoS ONE 9(2):1–9.

Fernandes R, Nadeau MJ, Grootes PM. 2012. Macronutrient-based model for dietary carbon routing in bone collagen and bioapatite. Archaeological and Anthropological Sciences, 4(4):291–301.

Fonseca G, Netto SA. 2006. Shallow sublittoral Benthic communities of the Laguna estuarine system, South Brazil. Brazilian Journal of Oceanography 54(1):41–54.

Fornari M, Giannini PCF, Junior DRN. 2012. Facies associations and controls on the evolution from a coastal bay to a lagoon system, Santa Catarina Coast, Brazil. Marine Geology 323: 56–68.

Fossile T, Ferreira J, da Rocha Bandeira D, Figuti L, Dias-da-Silva S, Hausmann N, Robson HK, Orton D, Colonese AC. 2019. Pre-Columbian fisheries catch reconstruction for a subtropical estuary in South America. Fish and Fisheries 20(6):1124–1137.

Friedman G. 1959. Identification of carbonate minerals by staining methods. Journal of Sedimentary Petrology 29(1):87–97.

Galetti M, Rodarte RR, Neves CL, Moreira M, Costa-Pereira R. 2016. Trophic niche differentiation in rodents and marsupials revealed by stable isotopes. PLoS ONE 11(4):1–15.

Gaspar M, DeBlasis P, Fish S, Fish P. 2008. Sambaqui (shell mound) societies of coastal Brazil. In: Silverman H, Isbell W, editors. Handbook of South American archaeology. Springer. p. 319–335.

Gavin DG. 2001. Estimation of inbuilt age in radiocarbon ages of soil charcoal for fire history studies. Radiocarbon 43(1):27–44.

Giannini PC. 2002. Complexo lagunar centro-sul catarinense-valioso patrimônio sedimentológico, arqueológico e histórico. Sítios geológicos e paleontológicos do Brasil 75:213–222.

Giannini PCF. 1993. Sistemas deposicionais no Quaternário Costeiro entre Jaguaruna e Imbituba, SC [doctoral thesis]. Universidade de São Paulo. doi: 10.11606/T.44.1993.tde-11032013-133424.

Giannini PC, Sawakuchi AO, Martinho CT, Tatumi SH. 2007. Eolian depositional episodes controlled by Late Quaternary relative sea level changes on the Imbituba–Laguna coast (southern Brazil). Marine Geology 237(3–4):143–168.

Giannini PCF, Villagran XS, Fornari M, Nascimento DRD Jr, Menezes PML, Tanaka APB, et al. 2010. Interações entre evolução sedimentar e ocupação humana pré-histórica na costa centro-sul de Santa Catarina, Brasil. Boletim do Museu Paraense Emílio Goeldi. Ciências Humanas 5(1):105–128.

Gillespie R. 1984. Radiocarbon user's handbook. Oxford: Oxford University Committee for Archaeology. Oxbow Books. ISBN 0 947816 93 8.

Goh K, Molloy B. 1972. Reliability of radiocarbon dates from buried charcoals. In: Proceedings of the 8th International Conference on Radiocarbon Dating, Wellington. The Royal Society of New Zealand.

Gruber N, Keeling C, Bacastow R, Guenther P, Lueker T, Wahlen M, Meijer H, Mook W, Stocker T. 1999. Spatiotemporal patterns of carbon-13 in the global surface oceans and the oceanic Suess effect. Global Biogeochemical Cycles 13(2):307–335.

Guerra AT. 1950. Contribuição ao estudo da geomorfologia e do quaternário do litoral de Laguna (Santa Catarina). Revista Brasileira de Geografia 12(4):535–564.

Heaton TJ, Köhler P, Butzin M, Bard E, Reimer RW, Austin WE, Ramsey CB, Grootes PM, Hughen KA, Kromer B, Reimer PJ. 2020. Marine20— the marine radiocarbon age calibration curve (0–55,000 cal BP). Radiocarbon 62(4):779–820.

Hedges RE, Reynard LM. 2007. Nitrogen isotopes and the trophic level of humans in archaeology. Journal of Archaeological Science 34:1240–1251.

Hellevang H, Aagaard P. 2015. Constraints on natural global atmospheric CO_2 fluxes from 1860 to 2010 using a simplified explicit forward model. Scientific Reports 5(June):1–12.

Hogg AG, Heaton TJ, Hua Q, Palmer JG, Turney CS, Southon J, Bayliss A, Blackwell PG, Boswijk G, Ramsey CB, Pearson C. 2020. SHCal20 Southern Hemisphere calibration, 0–55,000 years cal BP. Radiocarbon 62(4):759–778.

Jim S, Jones V, Ambrose SH, Evershed RP. 2006. Quantifying dietary macronutrient sources of carbon for bone collagen biosynthesis using natural abundance stable carbon isotope analysis. British Journal of Nutrition 95(06):1055.

Kjerfve B. 1994. Coastal lagoons. In: Kjerfve B, editor. Coastal Lagoon Processes. Elsevier.

Klokler DM. 2008. Food for body and soul: mortuary ritual in shell mounds (Laguna-Brazil) [PhD thesis]. The University of Arizona.

Klokler DM. 2012. Consumo ritual, consumo no ritual: festins funerários e sambaquis. Habitus 10(1):83–104.

Klokler DM. 2014. Adornos em concha do sítio cabeçuda. Revista de Arqueologia 27(2):150–169.

Klokler D. 2016. A fauna do sambaqui cabeçuda: 65 anos depois. In: III Encontro Latinoamericano de Zooarqueologia (ELAZ).

Klokler D. 2017. Shelly coast: constructed seascapes in southern Brazil. Hunter Gatherer Research 3(1):87–105.

Klokler D, Gaspar MD, Scheel-Ybert R. 2018. Why clam? Why clams? Shell mound construction in Southern Brazil. Journal of Archaeological Science: Reports 20:856–863.

Kneip A, Farias DS, DeBlasis P. 2018. Longa duração e territorialidade da ocupação sambaquieira na laguna de Santa Marta, Santa Catarina. Revista de Arqueologia 31(1): 25–51.

LeGrande AN, Schmidt GA. 2006. Global gridded data set of the oxygen isotopic composition in

seawater. Geophysical Research Letters 33(12): 1–5.

Leonel R, Magalhães A, Lunetta J. 1983. Sobrevivência de Anomalocardia brasiliana (Gmelin, 1791) (Mollusca: Bivalvia), em diferentes salinidades.". Boletim de Fisiologia Animal 7:63–72.

Libby W. 1954. Radiocarbon dating. American Scientist 44(1):98–112.

Lima TA. 2000. Em busca dos frutos do mar: os pescadores-coletores do litoral centro-sul do Brasil. REVISTA USP (44):270–327.

Longin R. 1971. New method of collagen extraction for radiocarbon dating. Nature 230(5291):241–242.

Ludemann T, Michiels HG, Nölken W. 2004. Spatial patterns of past wood exploitation, natural wood supply and growth conditions: iIndications of natural tree species distribution by anthracological studies of charcoal-burning remains. European Journal of Forest Research 123(4):283–292.

Macario KD, Alves EQ, Chanca IS, Oliveira FM, Carvalho C, Souza R, Aguilera O, Tenório MC, Rapagnã LC, Douka K, et al. 2016. The Usiminas shellmound on the Cabo Frio Island: marine reservoir effect in an upwelling region on the coast of Brazil. Quaternary Geochronology 35:36–42.

Macario KD, Alves EQ, Belém AL, Aguilera O, Bertucci T, Tenório MC, Oliveira FM, Chanca IS, Carvalho C, Souza R. 2018. The marine reservoir effect on the coast of Rio de Janeiro: deriving ΔR values from fish otoliths and mollusk shells. Radiocarbon 60(4):1151–1168.

Macario KD, Oliveira FM, Carvalho C, Santos GM, Xu X, et al. 2015a. Advances in the graphitization protocol at the Radiocarbon Laboratory of the Universidade Federal Fluminense (LAC-UFF) in Brazil. Nuclear Instruments Methods Physics Research Section B 361.

Macario KD, Oliveira FM, Moreira VN, Alves EQ, Carvalho C, et al. 2017. Optimization of the amount of zinc in the graphitization reaction for radiocarbon AMS measurements at LAC-UFF. Radiocarbon 59(3):885–891

Macario KD, Souza RCCL, Aguilera OA, Carvalho C, Oliveira FM, Alves EQ, Chanca IS, Silva EP, Douka K, Decco J. 2015b. Marine reservoir effect on the Southeastern coast of Brazil: results from the Tarioba shellmound paired samples. Journal of environmental radioactivity, 143:14–19.

Macario KD, Scheel-Ybert R, Ribeiro-Pinto N, Pereira BB, Amaral D, Alves EQ. 2021. Amourins shellmound: uncovering biodiversity and chronology through charcoal analyses. Radiocarbon 63(4):1085–1102.

Macario KD, Tenório MC, Alves EQ, Oliveira FM, Chanca IS, Netto B, Carvalho C, Souza R, Aguilera O, Guimarães RB. 2017. Terrestrial mollusks as chronological records in Brazilian shellmounds. Radiocarbon 59(5):1561–1577.

Mangerud, J. 1972. Radiocarbon dating of marine shells including a discussion of the apparent age of recent shells from Norway. Boreas 1(l): 143–172.

McFadgen B. 1982. Dating New Zealand archaeology by radiocarbon. New Zealand Journal of Science 25:379–392.

McGregor HV, Gagan MK. 2003. Diagenesis and geochemistry of Porites corals from Papua New Guinea: implications for paleoclimate reconstruction. Geochimica et Cosmochimica Acta 67(12):2147–2156.

Mendonça de Souza S. 1995. Estresse, doença e adaptabilidade. In: Congresso da Sociedade de Arqueologia Brasileira.

Metcalfe C, Chalk L. 1950. Anatomy of the dicotyledons. Vol. 2. Oxford, London: The Clarendon Press.

Milheira R, Macario K, Chanca I, Alves E. 2017. Archaeological earthen mound complex in the Patos Lagoon, southern Brazil: chronological model and freshwater influence. Radiocarbon 59(1):195–214.

Monti D, Frenkiel L, Moueza M. 1991. Demography and growth of Anomalocardia Brasiliana (Gmelin) (Bivalvia: Veneridae) in a Mangrove, in Guadeloupe (French West Indies). Journal of Molluscan Studies 57:249–257.

Moskal-del Hoyo M. 2013. Mid-Holocene forests from Eastern Hungary: new anthracological data. Review of Palaeobotany and Palynology 193:70–81.

Naito YI, Chikaraishi Y, Ohkouchi N, Mukai H, Shibata Y, Honch NV, Dodo Y, Ishida H, Amano T, Ono H, Yoneda M. 2010. Dietary reconstruction of the Okhotsk culture of Hokkaido, Japan, based on nitrogen composition of amino acids: implications for correction of ^{14}C marine reservoir effects on human bones. Radiocarbon 52(2):671–681.

Nascimento DRD Jr. 2010. Evolução sedimentar holocênica do delta do Rio Tubarão, estado de Santa Catarina [doctoral dissertation]. Universidade de São Paulo.

O'Connell TC, Kneale CJ, Tasevska N, Kuhnle GG. 2012. The diet-body offset in human nitrogen isotopic values: a controlled dietary study. American Journal of Physical Anthropology 149(3):426–434.

Oliveira F, Macario K, Carvalho C, Moreira V, Alves EQ, Chanca I, Diaz M, et al. 2021. LAC-UFF status report: current protocols and recent developments. Radiocarbon 63(4):1233–1245.

Pezo-Lanfranco L, Eggers S, Petronilho C, Toso A, da Rocha Bandeira D, Von Tersch M, dos Santos AMP, Ramos da Costa B, Meyer R, Colonese AC. 2018. Middle Holocene plant cultivation on the Atlantic Forest coast of Brazil? Royal Society Open Science 5:180432.

Pimenta FM, Campos EJD, Miller JL, Piola AR. 2005. A numerical study of the Plata River

plume along the southeastern South American continental shelf. Brazilian Journal of Oceanography 53(3–4):129–146.

Piola AR, Campos EJ, Möller Jr OO, Charo M, Martinez C. 2000. Subtropical shelf front off eastern South America. Journal of Geophysical Research: Oceans: 105(C3):6565–6578.

Piola AR, Romero SI. 2004. Analysis of space-time variability of the Plata River Plume. Gayana (Concepción) 68(2):482–486.

Piola AR, Matano RP, Palma ED, Möller Jr OO, Campos EJ. 2005. The influence of the Plata River discharge on the western South Atlantic shelf. Geophysical Research Letters 32(1).

Reid RP, Macintyre IG. 1998. Carbonate recrystallization in shallow marine environments: a widespread diagenetic process forming micritized grains. Journal of Sedimentary Research 68(5):928–946.

Rieth TM, Hunt TL, Lipo C, Wilmshurst JM. 2011. The 13th century Polynesian colonization of Hawai'i Island. Journal of Archaeological Science 38(10):2740–2749.

Rios E. 1994. Seashells of Brazil. Editora Fundação Universidade do Rio Grande, Rio Grande.

Rodrigues A, Borges-Azevedo C, Costa R, Henry-Silva G. 2013. Population structure of the bivalve Anomalocardia brasiliana, (Gmelin, 1791) in the semi-arid estuarine region of northeastern Brazil. Brazilian Journal of Biology 73(5):819–833.

Rodrigues-Carvalho C, Mendonça de Souza SM. 1998. Uso de adornos labiais pelos construtores do sambaqui de Cabeçuda, Santa Catarina, Brasil: Uma hipótese baseada no perfil dento-patológico. Revista de Arqueologia 11:43–55.

Rodrigues-Carvalho C, Scheel-Ybert R, Gaspar M, Bianchini GF, Klokler DM, Andrade MN, Borges DD. 2011. Cabeçuda-II: um conjunto de amoladores-polidores evidenciado em Laguna, SC. Revista do Museu de Arqueologia e Etnologia (21):401–405.

Rohr, J. 1961. Pesquisas paleoetnográficas na Ilha de Santa Catarina e notícias prévias sobre sambaquis da Ilha de São Francisco do Sul. Pesquisas 12: 1–18.

Russell N, Cook GT, Ascough PL, Scott EM, Dugmore AJ. 2011. Examining the inherent variability of ΔR: new methods of presenting ΔR values and implications for MRE studies. Radiocarbon 53(2):277–288.

Scheel-Ybert R. 2001. Man and vegetation in southeastern Brazil during the Late Holocene. Journal of Archaeological Science 28:471–480.

Scheel-Ybert R. 2020. Anthracology (charcoal analysis) In: Smith C, editor. Encyclopedia of global archaeology. New York/EUA: Springer-Verlag.

Scheel-Ybert R. 2016. Charcoal collections of the world. IAWA Journal 37:489–505.

Scheel-Ybert R, Rodrigues-Carvalho C, DeBlasis P, Gaspar M, Klokler DM. 2020. Mudanças e permanências no Sambaqui de Cabeçuda (Laguna, SC. Revista de Arqueologia 33:169–197.

Scheel-Ybert R, Boyadjian C. 2020. Gardens on the coast: Considerations on food production by Brazilian shellmound builders. Journal of Anthropological Archaeology 60:101–211.

Schiffer MB. 1986. Radiocarbon dating and the "old wood" problem: the case of the Hohokam chronology. Journal of Archaeological Science 13(1):13–30.

Schoeninger MJ, DeNiro MJ. 1984. Nitrogen and carbon isotopic composition of bone collagen from marine and terrestrial animals. Geochimica et Cosmochimica Acta 48(4):625–639.

Schoeninger MJ, DeNiro MJ, Tauber H. 1983. Stable nitrogen isotope ratios of bone collagen reflect marine and terrestrial components of prehistoric human diet. Science (New York):1381–1383.

Schwarcz HP, Melbye J, Katzenberg M, Knyf M. 1985. Stable isotopes in human skeletons of southern Ontario: reconstructing Palaeodiet. Journal of Archaeological Science 12(3):187–206.

Sepulcre S, Durand N, Bard E. 2009. Mineralogical determination of reef and periplatform carbonates: calibration and implications for paleoceanography and radiochronology. Global and Planetary Change 66(1–2):1–9.

Sigman DM, Boyle EA. 2000. Glacial/interglacial variations in atmospheric carbon dioxide. Nature 407:859–869.

Stuiver M, Polach HA. 1977. Reporting of ^{14}C data. Radiocarbon 19(3):355–363.

Stuiver M, Pearson G, Braziunas T. 1986. Radiocarbon age calibration of marine samples back to 9000 cal yr BP. Radiocarbon 28: 980–1021.

Tagliabue A, Bopp L. 2008. Towards understanding global variability in ocean carbon-13. Global Biogeochemical Cycles 22(1):1–13.

Tanaka APB, Giannini PCF, Fornari M, Nascimento DR Jr, Sawakuchi AO, Rodrigues SI, Menezes PML, DeBlasis P, Porsani JL. 2009. A planície costeira holocênica de Campos Verdes (Laguna, SC): evolução sedimentar inferida a partir de georradar (GPR), granulometria e minerais pesados. São Paulo, Revista Brasileira de Geociências 39(4): 750–766.

Taylor RE. 1987. Radiocarbon dating: an archaeological perspective.

Toby BH, Von Dreele RB. 2013. GSAS-II: the genesis of a modern open-source all-purpose crystallography software package. Journal of Applied Crystallography 46(2):544–549.

Toniolo, T, Giannini PCF, Angulo RJ, de Souza MC, Pessenda LCR, Spotorno-Oliveira P. 2020. Sea-level fall and coastal water cooling during the Late Holocene in southeastern Brazil based on vermetid bioconstructions. Marine Geology 428:106281.

Toso A, Hallingstad E, McGrath K, Fossile T, Conlan C, Ferreira J, da Rocha Bandeira D, Giannini PCF, Gilson SP, de Melo Reis Bueno L, Bastos MQR. 2021. Fishing intensification as response to Late Holocene socio-ecological instability in southeastern South America. Scientific Reports 11(1):1–14.

Tucker M, Wright V. 1990. Carbonate sedimentology. Oxford: Blackwell Science.

Van de Merwe N. 1982. Carbon isotopes, photosynthesis, and archaeology. American Scientist 70(6):596–606.

van Klinken G. 1999. Bone collagen quality indicators for paleodietary and radiocarbon measurements. Journal of Archaeological Sciences 26(6):687–695.

Vernet J. 1999. Reconstructing vegetation and landscapes in the Mediterranean: the contribution of anthracology. In: Environmental reconstruction in Mediterranean landscape archaeology. p. 25–33.

Villagran XS, Giannini PC. 2014. Shell mounds as environmental proxies on the southern coast of Brazil. Holocene 24(8):1009–1016.

Wagner G, Hilbert K, Bandeira D, Tenório MC, Okumura MM. 2011. Sambaquis (shell mounds) of the Brazilian coast. Quaternary International 239:51–60.

Walker PL, DeNiro MJ. 1986. Stable nitrogen and carbon isotope ratios in bone collagen as indices of prehistoric dietary dependence on marine and terrestrial resources in Southern California. American Journal of Physical Anthropology 71(1):51–61.

Waterbolk HT. 1971. Working with radiocarbon dates. Proceedings of the Prehistoric Society 37(2):15–33.

Webb GE, Price GJ, Nothdurft LD, Deer L, Rintoul L. 2007. Crytic meteoric diagenesis in freshwater bivalves: implications for radiocarbon dating. Geology 35(9):803–806.

Webb EC, Lewis J, Shain A, Kastrisianaki-Guyton E, Honch NV, Stewart A, Miller B, Tarlton J, Evershed RP. 2017. The influence of varying proportions of terrestrial and marine dietary protein on the stable carbon-isotope compositions of pig tissues from a controlled feeding experiment. Science and Technology of Archaeological Research 3(1):28–44.

Wilmshurst JM, Hunt TL, Lipo CP, Anderson AJ. 2011. High-precision radiocarbon dating shows recent and rapid initial human colonization of East Polynesia. Proceedings of the National Academy of Sciences 108(5):1815–1820.

Xu X, Trumbore SE, Zheng S, Southon JR, McDuffee KE, Luttgen M, Liu JC. 2007. Modifying a sealed tube zinc reduction method for preparation of AMS graphite targets: reducing background and attaining high precision. Nuclear Instruments and Methods in Physics Research, Section B: Beam Interactions with Materials and Atoms 259:320–329.